



Decoherence Induced by a Quenching Driven Field on the Motion of a Single Electron

L. C. Fai^{1,2}, M. Tchoffo^{1*}, J. T. Diffo³ and G. C. Fouokeng¹.

¹Mesoscopic and Multilayer Structures Laboratory, Department of Physics, Faculty of Science, University of Dschang, Dschang, Cameroon.

²Department of Physics, Higher Teachers' Training College, University of Bamenda, Cameroon.

³Department of Physics, Higher Teachers' Training College, University of Maroua, Cameroon.

Authors' contributions

This work was carried out in collaboration between all authors. Authors LCF and MT designed the study, managed the literature searches, wrote the first and final drafts of the manuscript. Author GCF performed simulations. Author JTD helped in writing of the final draft. All authors read and approved the final manuscript.

Original Research Article

Received 9th May 2013
Accepted 25th September 2013
Published 24th October 2013

ABSTRACT

We investigate the motion of an electron in a one dimensional crystal coupled to an EMF potential, driven by an external force which is continuously switched on and off. The Shannon entropy and the thermodynamic parameters of the system are evaluated using the density matrix and the statistical sum, through the Feynman path integral method. The coupling with the system and its environment (modelised here by the quenching field) inducing decoherence. That effect is reduced when the magnetic confinement frequency increases.

Keywords: *Quenching; Decoherence; Magnetic confinement frequency; thermodynamic parameters.*

*Corresponding author: Email: mtchoffo2000@yahoo.fr;

1. INTRODUCTION

Quantum decoherence, where coherence in a quantum system is reduced due to interaction with its environment is a fundamental and complicated concept of physics. Decoherence refers to the destruction of a quantum interference pattern and is relevant to the many experiments that depend on achieving and maintaining entangled states. Examples of such efforts are in the areas of quantum teleportation [1], quantum information and computation [2, 3], entangled states [4], Schrödinger cats [5], and the quantum-classical interface [6]. For an overview of many of the interesting experiments involving decoherence, we refer to [4, 7-11]. Coherent manipulation and storage of quantum information are required in order to construct a working quantum computer and rely on reducing decohering interaction between its basic elements, the qubits, and their environment. The application of a magnetic field potential as confining potential to solids have provided recently valuable information on electron spin dynamics and decoherence in quantum computing [11]. After the pioneering work on the information theory by Shannon [12], many studies have been carry out on the question of how information storage, processing and transmission tasks can be performed with macroscopic decohered resources [13,14]. All thermodynamic quantitative tools such as entropy and specific heat capacity applied perfectly in the quantum domain require that, one should focus on a single type of information associated with a particular measurement on the quantum system [15]. The difference between quantum information with its classical counterpart has been mathematically defined using thermodynamic quantities [16, 17]. The Shannon entropy given by the classical information theory can be negative when considering quantum entangled systems [18, 19].

The thermodynamic properties of electron in a system without a magnetic confinement, driven by a constant force have been discussed in the literature [20-22]. These quantities are used to characterize the lost of information showing decoherence phenomenon related to evolving pure quantum states [12, 22, 23]. Indeed, it is known that the external force enhances disorder in the system by increasing its entropy as compared to the motion of a simple harmonic oscillator [24].

The simplest way of analyzing decoherence in a motion of single electron is to evaluate the electronic density and the partition function of the system; because once both functions are known, their thermodynamic properties can then be obtained.

In this paper, our objective is to show the effect of the magnetic field potential on the thermodynamic quantitative tools and decoherence tailoring of a single electron driven by a quenching field, using the path integral method. The organization of the paper is as followed; in section 2 we explain the fundamental definitions needed for the comprehension of the decoherence phenomenon as well as its formulation for the case of this investigation. The nature of the external on/off force is given and the electronic density through the Feynman path integral method is found. In section 3, the Shannon entropy is determined in the case of simple and double Gaussian wave packet. In sections 4, we evaluate the statistical sum which helps to establish the thermodynamic parameters of the system, such as the internal energy, the specific heat capacity and the Boltzmann entropy. Finally in section 5 a brief discussion and concluding remarks are presented.

2. FUNDAMENTAL DEFINITIONS

The problem of decoherence in a classical and quantum systems has been extensively studied [4,7, 25-28]. In this work, we consider the system with the following Hamiltonian:

$$H = H_a - e \varphi + f(t) x \tag{2.1}$$

where H_a , $e\varphi$ are respectively the Hamiltonian of non-bonded electron in a magnetic field potential and the electric field potential. $f(t)$ is an arbitrary function of time that is modeled to characterize the coupling between the harmonic oscillator ($H_a - e \varphi$) and the classical pump.

Considering the electron system with s degrees of freedom and using the non-negative time dependent phase space density function of the system noted by $v(\mathbf{x}, t) = v(\mathbf{x}_1, \mathbf{x}_2, \dots, \mathbf{x}_s, t)$, obeying the normalization condition,

$$\int v(\mathbf{x}, t) d\mathbf{x} = 1 \tag{2.2},$$

and associated to the Gibbs-Shannon entropy relation

$$S_{GSE}(t) = -\frac{1}{N!} \int v(\mathbf{x}, t) \ln(\hbar^s v(\mathbf{x}, t)) d\mathbf{x}. \tag{2.3},$$

with $\hbar = 1$, the Shannon entropy for the state given by the wave function $\psi(x, t)$ leads to

$$S_{SE}(t) = -\int |\psi|^2 \ln|\psi(\mathbf{x}, t)|^2 d\mathbf{x} \tag{2.4}.$$

This relation is obtained with the help of the Schrödinger wave equation in the Born interpretation [29], using the Leipnik entropy condition [18].

$$v(\mathbf{x}, t) = |\psi(\mathbf{x}, t)|^2 \geq 0 \tag{2.5}$$

To get the entire expression of the Shannon entropy given in Eq.(2.4), we use the following time dependent evolution operator

$$\mathcal{N}(\mathbf{x}'', t'', \mathbf{x}', t') = \int_{x'=x(t')}^{x''=x(t'')} D\mathbf{x}(t) \exp\{ i S_T(\mathbf{x}(t))/\hbar \} \tag{2.6}$$

where $D\mathbf{x}(t)$ is the measure, $S_T(\mathbf{x}(t)) = \int_0^t L(\mathbf{x}(u), \dot{\mathbf{x}}(u)) du$ the total action of the system and

L the Lagrangian of the system (for a more detailed analysis, see Ref. [30]). The evolution operator is related to the time dependent Schrödinger's wave function through Eq.(2.7)

$$\mathcal{N}(\mathbf{x}'', t'', \mathbf{x}', t') = \int_{\mathbf{x}'}^{\mathbf{x}''} d\mathbf{x} \psi_s^*(\mathbf{x}, t) \psi_s(\mathbf{x}, t) \quad (2.7).$$

In the semi-classical approximation, the time evolution operator (2.7) called the propagator reads:

$$\mathcal{N}(\mathbf{x}'', t'', \mathbf{x}', t') = \left[\frac{i}{\hbar} \frac{\partial^2}{\partial \mathbf{x}' \partial \mathbf{x}''} S_{cl}(\mathbf{x}'', t'', \mathbf{x}', t') \right]^{\frac{1}{2}} \exp \left\{ \frac{i}{\hbar} S_{cl}(\mathbf{x}'', t'', \mathbf{x}', t') \right\} \quad (2.8)$$

where S_{cl} is a classical action given by [30, 31]

$$\begin{aligned} S_{cl} = & \frac{m\Omega}{2 \sin(\Omega t)} \left[(x_i^2 + x_f^2) \cos(\Omega T) - 2x_i x_f \right] + \frac{x_f}{\sin(\Omega t)} \int_0^t \sin(\Omega u) f(u) du \\ & + \frac{x_i}{\sin(\Omega t)} \int_0^t \sin(\Omega(t-u)) f(u) du \\ & - \frac{1}{m\Omega \sin(\Omega t)} \int_0^t dt \int_0^t du \sin(\Omega u) \sin(\Omega(t-\tau)) f(\tau) f(u) \end{aligned} \quad (2.9).$$

In Eq.(2.9), the following quantities m , Ω , x_i and x_f are respectively the electron mass, the electromagnetic frequency, the initial and final displacements. In the following sections, to explain the decoherence observation; we have evaluated the Shannon entropy as well as the electron's thermodynamic properties in a Gibbs ensemble.

3. SHANNON ENTROPY

From the Hamiltonian given in Eq.(2.1), using the canonical transformation, the Lagrangian of the system reads:

$$L(\mathbf{x}, \dot{\mathbf{x}}, t) = \frac{1}{2m} \left(\mathbf{P} + \frac{e}{c} \mathbf{A}(x) \right)^2 + \frac{1}{2} m \Omega_0^2 x^2 + f(t) x \quad (3.1)$$

where Ω_0 is the frequency of the electric field and

$$\mathbf{A}(x) = \frac{1}{2} \mathbf{H} \wedge \mathbf{x} \quad (3.2)$$

is the magnetic field potential vector. For the incoming light (with photon of energy $\hbar\omega$) of the relatively low intensity and within the coulomb Gauge, Eq. (3.2) is rewritten as the interaction potential by introducing the substitution

$$V_{int} = \frac{I}{2} m \left(\frac{\omega_c}{2} \right)^2 x^2 \tag{3.3}$$

In Eq.(3.3) ω_c represents the cyclotron frequency. Considering the frequency of the entire system as

$$\Omega^2 = \Omega_0^2 + \frac{\omega_c^2}{4} \tag{3.4},$$

and considering Eqs.(3.3) and (3.4), Eq. (3.1) becomes

$$L(\mathbf{x}, \dot{\mathbf{x}}, t) = \frac{m \dot{\mathbf{x}}^2}{2} - \frac{1}{2} m \Omega^2 x^2 + f(t)x \tag{3.5}.$$

Using the Euler-Lagrange equations, Eq.(3.5) obeys the following differential equation

$$m \ddot{x} + m \Omega^2 x = f(t) \tag{3.6}$$

Equation.(3.6) has previously been solved to study the decoherence phenomenon in a dissipative harmonic oscillator with several methods such as the reduced density matrix [10,32]. Using the Feynman path integral method, the classical action along the classical path is found as follows:

$$S_{cl} = S_{cl}^0 + \frac{x_f}{\sin(\Omega t)} \mathcal{A}_1 + \frac{x_i}{\sin(\Omega t)} \mathcal{A}_2 - \frac{1}{m \Omega \sin(\Omega t)} \mathcal{A}_3 \tag{3.7}$$

with

$$S_{cl}^0 = \frac{m\Omega}{2 \sin(\Omega t)} \left[(x_i^2 + x_f^2) \cos(\Omega t) - 2x_i x_f \right] \tag{3.8}$$

being the action of the free harmonic oscillator. The parameters \mathcal{A}_1 , \mathcal{A}_2 and \mathcal{A}_3 are the displacement coordinates given respectively by

$$\mathcal{A}_1 = \int_0^t \sin(\Omega \tau) f(\tau) d\tau \tag{3.9}$$

$$\mathcal{A}_2 = \int_0^t \sin(\Omega(t - \tau)) f(\tau) d\tau \tag{3.10}$$

$$\mathcal{A}_3 = \int_0^t d\tau \int_0^\tau \sin(\Omega u) \sin(\Omega(t - \tau)) f(\tau) f(u) du \tag{3.11}$$

Considering Eqs (3.9) to (3.11), the propagator (2.8) representing the transition amplitude of the electron leads to

$$\aleph(x_f, t; x_i, 0) = \left\{ \frac{m\Omega}{2\pi i \hbar \sin(\Omega t)} \right\}^{1/2} \cdot \exp \left\{ i \frac{m\Omega}{2\hbar \sin(\Omega t)} [(x_i^2 + x_f^2) \cos(\Omega t) - 2x_i x_f] \right\} \quad (3.12).$$

In the limiting case where the external field is neglected, i.e. $\Delta_1 = \Delta_2 = \Delta_3 = 0$, we recover the well-known statistical sum of a free harmonic oscillator [33].

$$Z_0 = 1/(2 \sinh(\lambda \hbar \Omega / 2)) \quad (3.13).$$

Now, to facilitate the resolution of the problem, using the Green's function G [26], relation (3.9) becomes

$$\Delta = x_d(t) = \int_0^t G(t - \tau) f(\tau) d\tau \quad (3.14)$$

and from where we deduce (3.15) and (3.16)

$$\Delta = \frac{1}{m \Omega} \int_0^t \sin(\Omega(t - \tau)) f(\tau) d\tau \quad (3.15)$$

$$\Delta_2 = m \Omega \Delta \quad (3.16).$$

To determine the entropy and the specific heat capacity, we start by looking for the probability distribution density in space coordinates.

$$P(x, t) = |\psi(x, t)|^2 \quad (3.17)$$

$$\psi(x, 0) = (2\pi\sigma^2)^{-1/4} \exp\{-x^2/4\sigma^2\} \quad (3.18)$$

$$\Psi(x', 0) = (8\pi\sigma^2)^{-1/4} \ell \left[\exp\{-(x' - d/2)^2/4\sigma^2\} + \exp\{-(x' + d/2)^2/4\sigma^2\} \right] \quad (3.19)$$

where $\ell = \sqrt{1/2(1 + \exp\{-d^2/8\sigma^2\})}$ is the normalization factor and d represents the distance between the top of the two waves in the double Gaussian state; $\sigma^2 = \hbar/2m\Omega$. The time dependent wave functions are respectively expressed in terms of the propagator as

$$\psi(x, t) = \int \aleph(x_f, t_f; x_i, 0) \psi(x, 0) dx \quad (3.20)$$

Eqs. (3.18) and (3.19) designate the Gaussian centered at the mean position of the particle at time $t = 0$ with the variance σ . Without loss of generality, we take $x_i = 0$.

Hereafter, we apply a driven external force as a switching protocol in which the source is turned on and off for a finite time [34],

$$f(t) = \begin{cases} f_0 \sin(\Omega t) & \text{if } 0 < t \leq \pi/\Omega \\ 0 & \text{otherwise} \end{cases} \quad (3.21)$$

In relation (3.21), f_0 is the amplitude of the driven force. Particularly, we assume in the present work that both the single electron system and the external force are in the resonance frequency Ω . Based on the information entropy definition

$$S_T = -K_B \sum_i^N P_i \ln P_i \quad (3.22)$$

and considering both single Gaussian and double Gaussian states, the time dependent entropy leads respectively to:

$$S_1 = \begin{cases} \frac{2K_B \sigma^2}{\sqrt{2\pi \sigma^2}} \Gamma(3/2) - K_B b^2 / \sigma^2 \ln(1/\sqrt{2\pi \sigma^2}) \exp\{-b^2/2\sigma^2\} & , \quad 0 < t \leq \pi/\Omega \\ 1/\sqrt{\pi} \Gamma(3/2) - 2K_B \ln(1/\sqrt{2\pi \sigma^2}) & , \quad \text{otherwise} \end{cases} \quad (3.23)$$

$$S_2 = -K_B/T_i \begin{cases} \wp + \Im + \diamond, & 0 < t \leq \pi/\Omega \\ \wp' + \Im' + \diamond', & \text{otherwise} \end{cases} , T_i = 1 + \exp(-d^2/8 \sigma^2) \quad (3.24)$$

In Eq. (3.24), by letting

$$C_1 = (b - d/4\sigma^2)^2; \quad Z_1 = d/2 \cos(\Omega t); \quad Y = f_0/m \Omega^2 [\Omega t \cos(\Omega t) - \sin(\Omega t)];$$

$$\gamma = 2\ell^2/\sqrt{2\pi \sigma^2} \quad , \quad \alpha = e^{-d^2 \cos^2 \theta / 8\sigma^2} ,$$

the quantities \wp' , \Im' , \diamond' are respectively expression in terms of \wp , \Im , \diamond in the absence of the external force and are given by:

$$\wp = \ln(\gamma) \exp\left\{-\frac{x^2 + 2Z_1^2 + Y^2}{2\sigma^2}\right\} [1 + \exp\{2 Z_1 Y/\sigma^2\}] + Z_1/\sigma^2 [1 + \cosh(Z_1/\sigma)^2] \quad (3.25)$$

$$\Im = 2 \alpha \cos^2(Y C_1) \exp\{-(\sigma C_1)^2/2\} [\ln(\gamma) + 2 Z_1^2 \gamma/\sigma^2] \quad (3.26)$$

$$\diamond = 2 \alpha \cos Z_1 C_1 \exp\{Z_1^2/2 \sigma^2 - (\sigma C_1)^2/2\} + 1 + \exp\{-(Z_1/\sigma)^2\} \quad (3.27).$$

Γ is gamma function and b is the diving factor due to the external force given as,

$$b = a_0 (\Omega t \cos(\Omega t) - \sin(\Omega t) / \Omega t) \quad (3.28)$$

Where $a_0(t) = \frac{f_0 t}{2 m}$ defining an attenuation coefficient. The driving factor b plotted in Fig.1 represents the principal factor that characterizes the coupling of the system with the driven field. This factor which contains all information about the coupling of the system is a usual factor of decoherence characteristic.

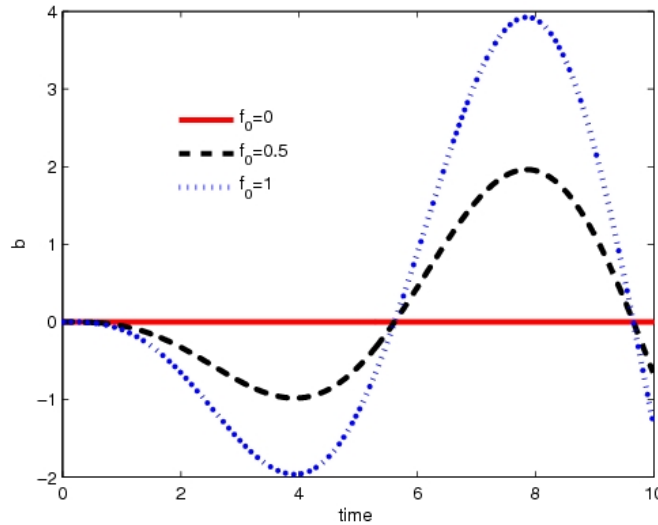


Fig. 1. Plot of decoherence driving factor versus time, for different values of the driven field intensity. The fact that the factor $b \rightarrow \infty$ when $f_0 \rightarrow \infty$ shows the increase of the decoherence in the system.

In accordance with the resolution of Eq. (3.28), this curve shows that the decoherence driving factor b displays different maxima and minima showing different bounded zones. Outside these zones $b \rightarrow 0$. These zones are the decoherence free regions. Obviously, the characteristic $b \rightarrow 0$, is also obtained for very low driven field frequency. Thus, in this consideration (i.e. $b \rightarrow 0$,) the entropy becomes independent of time. In Fig. 2, to describe the coherence of the system we plot the entropy S_0 versus the frequency Ω of the system for $b \rightarrow 0$ and the Shannon entropy S_0 is seen to decrease exponentially (i.e. $S_0 \rightarrow 0$). This property $S_0 \rightarrow 0$ is particular for the pure state system and thus to the coherence motion of the system.

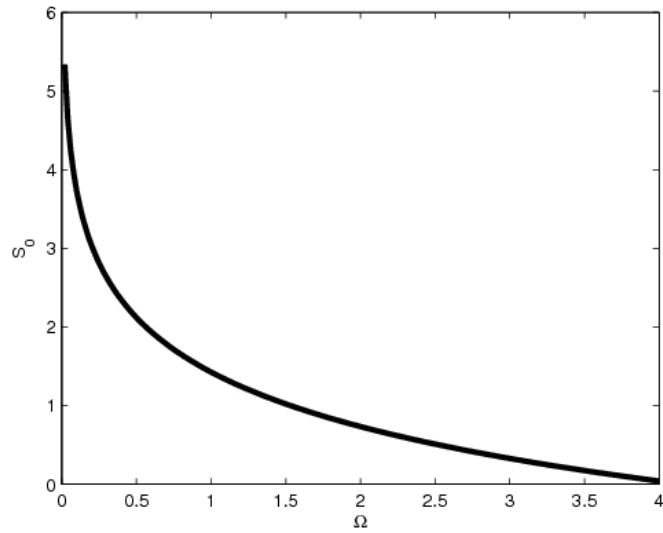


Fig. 2. Plot of the Variation of the Shannon entropy S_0 with respect to the field confinement Ω . This curve tends rigorously to zero for high frequency of the field and shows that the effect of the field confinement contributes to reduce decoherence.

The Shannon entropy for the single and double Gaussian wave packets are found theoretically and are given by Eqns. 3.23 and 3.24. These results are represented graphically by Figs. 3,4 and Fig. 5 with respect to time t and the induced factor b .

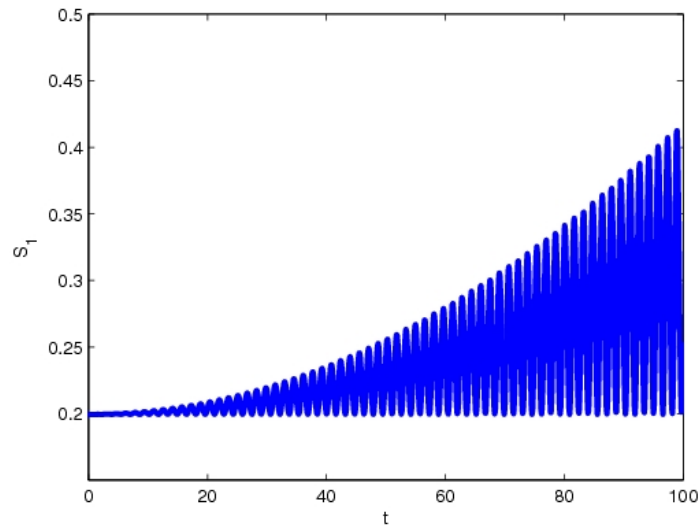


Fig. 3. plot of the Shannon entropy versus time in the case of single Gaussian wave packet.

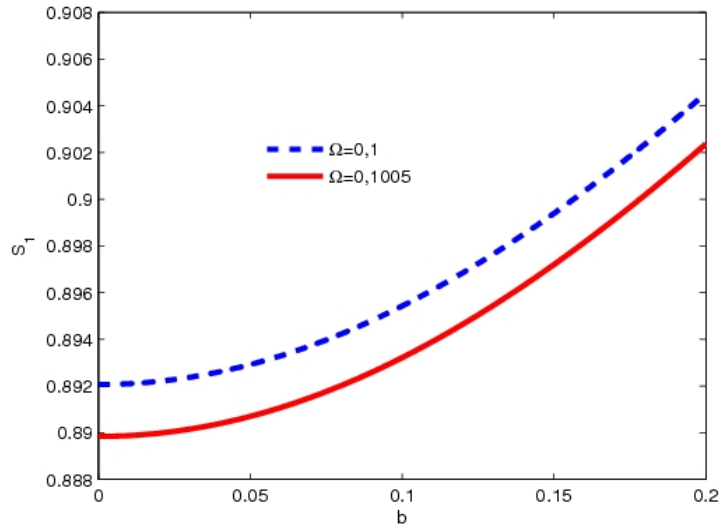


Fig. 4. plot of the Shannon entropy versus the driven factor b in the case of single Gaussian wave packet.

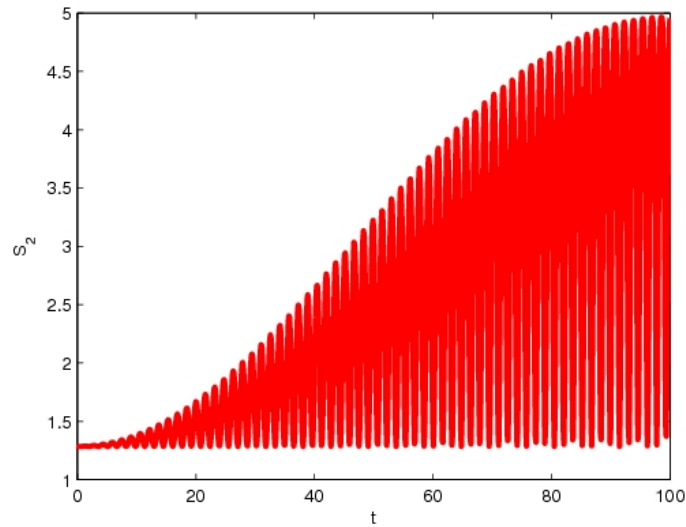


Fig. 5. plot of the Shannon entropy versus time in the case of double Gaussian wave packet.

These curves show that Shannon entropy increases when t and b is increased.

The temperature as a source of disorder induces the loss of the original information of the system when the later interacts with its environment. With the Feynman's statistical method, in the following section we will determine some thermodynamic parameters allowing us to evaluate the influence of the temperature on the decoherence of the system.

4. THERMODYNAMIC PARAMETERS AND DECOHERENCE.

According to the Feynman statistics, the thermodynamic parameters such as specific heat capacity, Boltzmann entropy can easily be calculated through the statistical sum by evaluating the free energy of the system.

The Lagrangian in (3.5) becomes

$$L(\dot{x}, x, -i\hbar\sigma) = \frac{m}{2} \dot{x}^2 - \frac{m \Omega^2}{2} x^2 + f(\sigma) x \quad (4.1)$$

Thus the propagator in (3.12) takes the following form:

$$\mathfrak{K}(x, x', -i\hbar\lambda) = \sqrt{\eta/\pi \hbar} \exp \{B_1 + B_2 + B_3 + B_4\} \quad (4.2)$$

where

$$B_1 = -\frac{\eta}{\hbar} [-2x_i x_f + (x_i^2 + x_f^2) \cosh(\hbar\Omega\lambda)] \quad (4.3a)$$

$$B_2 = -\frac{2\eta x_i}{m \hbar\Omega} \int_0^\lambda f(\sigma) \sinh(\hbar\Omega(\lambda - \sigma)) d\sigma \quad (4.3b)$$

$$B_3 = -\frac{2\eta x_f}{m \hbar\Omega} \int_0^\lambda f(\sigma) \sinh(\hbar\Omega) \sigma d\sigma \quad (4.3c)$$

$$B_4 = \frac{2\eta}{m^2 \hbar\Omega^2} \int_0^\lambda \int_0^\sigma f(\sigma) f(\sigma') \sinh(\hbar\Omega(\lambda - \sigma')) \sinh(\hbar\Omega) \sigma \sigma' d' d\sigma \quad (4.3d)$$

$$\eta = \frac{m \Omega}{2 \sinh(\Omega \lambda \hbar)} \quad (4.3e)$$

With relations (4.1) and (4.2), and assuming that the system is at the thermodynamic equilibrium with ordered energy microstates $\{E_n\}$, $n = 1, 2, \dots$, the partition function Z that encodes the probabilistic information about the system is

$$Z = \sum_{n=1}^{\infty} \exp\{-\beta E_n\} \quad (4.4)$$

Where the parameter $\beta = 1/K_b T$ represents the inverse temperature of the system. The form of (4.4) is reminiscent of the time-evolution constructed from the energy eigenstates back in Eqs.(3.19) and (3.20). These have an equivalent expression through the integral over propagators to all possible points. Hence, we replace the time t with the quantity $-i\beta$ and this operation moves us into the real part of the Euclidean path integrals.

Following the Feynman-Hibbs [30] methods, the partition function (4.4) becomes

$$Z = \int_{-\infty}^{+\infty} dx \mathfrak{K}(x', \beta\hbar, x) = \sum_n \langle n | \int_{-\infty}^{+\infty} dx \exp\{-\beta E_n |x\rangle \langle x| n\rangle\} = \sum_n \exp(-\beta E_n) \quad (4.5)$$

and thus

$$Z = Z_0 \exp\left\{A L^2/\hbar \left[D_0^2(\lambda - D_1)^2 + D_2(1/4 D_2 - \lambda D_0 + D_1 D_0)\right]\right\} \quad (4.6)$$

with $D_0 = \sinh^2(\hbar\Omega \lambda/2)$, $D_1 = 1/8 \hbar\Omega \sinh^2(\hbar\Omega \lambda/2)$ and

$$D_2 = 1/4 \hbar\Omega \sinh^3(\hbar\Omega \lambda).$$

Now, the various thermodynamic quantities can be found using the free energy

$$F = U - TS_b = -K_b T \ln Z \quad (4.7)$$

where $U = d \ln(Z/d\beta)$ represents the internal energy and $S_b = -dF/dT$ the Boltzmann entropy. In the microcanonical ensemble, the specific heat capacity at constant volume is defined by the relation $C_v = dU/dT$. In the high temperature regimes the following expressions are obtained

$$U = \alpha_0 T - \alpha_2 \left[3/4 - 3\Omega \alpha_1 / 2K_b - 3/4 T^2 - 3\alpha_1 \Omega^3 / 2K_b T^3 - 457/\hbar + 29\Omega^2 / 2T^2\right] + 39\alpha_2 / 8\hbar \quad (4.8)$$

$$C_v = \alpha_4 \left[3/4 - 3\beta^3 \Omega \alpha_3 / K_b - 9\beta^2 K_b^2 / 4 - 15\Omega^3 K_b^3 \beta^6 \alpha_3 / 2 - 457/\hbar - 87\Omega^2 K_b^2 / 2\right] - 39\alpha_4 / 8\hbar \quad (4.9)$$

$$S_b = \alpha_0 - \ln \hbar\Omega / T - \alpha_5 \left[3\hbar/4 - 3\Omega \hbar^3 / 2T - 3\hbar/4 T^2 - 3\hbar^3 \Omega^3 / 2T^4 + 29\hbar\Omega^2 / 2T^2 - 39/8 - 457\right] \quad (4.10)$$

where $\alpha_1 = \hbar^2 K_b / T$; $\alpha_2 = f_0^2 \alpha_1 / 8m$; $\alpha_3 = K_b^2 \hbar^2 / \beta^2$; $\alpha_4 = K_b f_0^2 \alpha_3 / 8m$; $\alpha_5 = f_0^2 \hbar K_b / 8m T^2$

according to the theoretical results obtained in Eqs.(4.8), (4.9) and (4.10) the curves presented in Figs. 6-8 are plotted in the unit of K_b .

Fig. 6 shows the dependence of the specific heat capacity on both external quenching field and temperature. Note that for high quenching field intensity, there exists a range of temperature where the specific heat capacity is slightly negative. This range of temperature corresponds to the domain where the system lost it energy to it environment.

Figs. 7 and 8 show consequently that the internal energy and the Boltzmann entropy increase when the temperature T and the driven quenching field intensity f_0 increases.

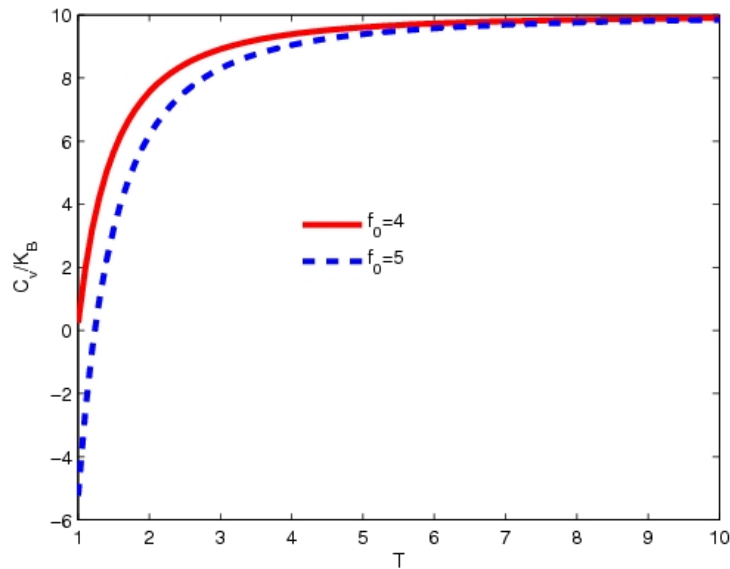


Fig. 6. plot of the Specific heat capacity C_v as a function of Temperature T , plotted for different value of the external field intensity f_0 .

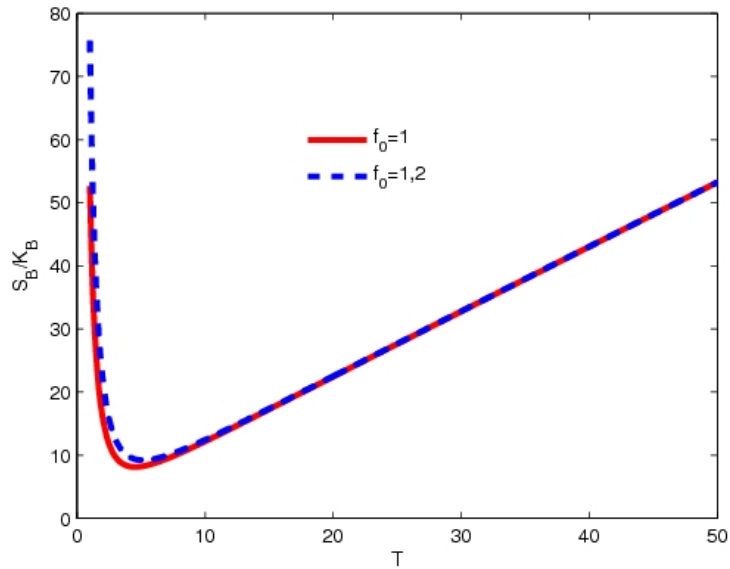


Fig. 7. plot of the Boltzmann entropy S_b as a function of Temperature T , plotted for different value of the external field intensity f_0 .

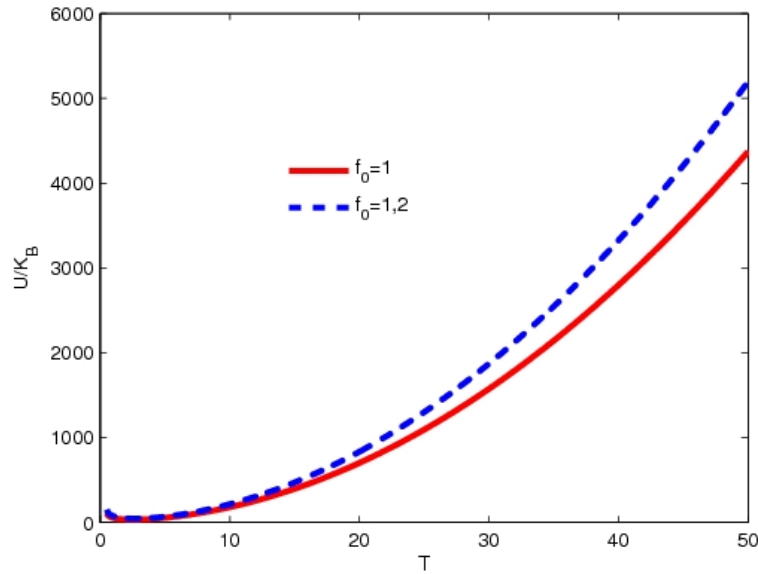


Fig. 8. plot of the Internal energy U as a function of Temperature T , plotted for different value of the external field intensity f_0

As it is already shown in the literature, we observed in the two principal parts of this work that, the environment (external periodic force in resonance with the harmonic oscillator) increases the entropy [35]. Taking into account the fact that the disorder induces decoherence and that the entropy is the main characteristic of disorder, we can say that the decoherence increases with the increase of the entropy of the system.

5. CONCLUSION

In this work, it is shown from the above that, the coupling with the environment (modelised here by the external quenching field) is described by the factor b . This factor that translates the interference term is characterized by the cosine factor. The later measures the disappearance of the interference term, that is, the loss of coherence (decoherence), by defining an attenuation coefficient $a(t)$, which is the factor multiplying the cosine. The results are presented for the resonant case, i.e. when the cyclotron frequency is equal to that of the quenching driven field. The Shannon entropy is evaluated, respectively for one and two Gaussian wave packet. The thermodynamic quantities such as the internal energy, the Boltzmann entropy, and the specific heat are calculated. The Shannon entropy increases with time and with the external quenching field intensity. The internal energy and the Boltzmann entropy increase with temperature and the external quenching field intensity, while the specific heat decreases. It is seen with the factor b and $a(t)$ that decoherence exist even in the absence of dissipation. This effect (decoherence) is reduced with the increase of the magnetic confinement.

ACKNOWLEDGEMENTS

We acknowledge the support from SDI. We thank also the reviewers for their contributions.

COMPETING INTERESTS

Authors have declared that no competing interests exist.

REFERENCES

1. Zeilinger A. *Sci. Am. Quantum Teleportation*. 2000;282(4):32-41.
2. Bennett CH. *Coupling and Entangling of Quantum States in Quantum Dot*. *Phys. Today*. 1995;48(10):24-30
3. Rogers P. *Quantum Information*. *Physics World-special issue*. 1998;11(3):33-57.
4. S.Haroche. *Entanglement, Decoherence and the Quantum/Classical Boundary*. *Phys. Today*, 1998; 51(7): 36-42.
5. Zeilinger A. *The Quantum Centennial*. *Nature*. 2000;408:639-641.
6. Tegmark M, Wheeler JA. *Decoherence in Phase Space - MAIK "Nauka/Interperiodica"*. *Sci. Am*. 2001;284(2):68-75.
7. Myatt CJ, King BE, Turchette QA, et al. *Decoherence of quantum superpositions through coupling to engineered reservoirs*. *Nature*. 2000;403:269-273.
8. Murakami M, Ford GW, O'Connell RF. *Decoherence in Phase Space*. *Laser Physics*. 2003;13(2):180–183.
9. O'Connell RF. *Decoherence in nanostructures and quantum systems*. *Physica E*. 2003;19:77–82.
10. Ratchov A, Faure F, Hekking FWJ. *Loss of quantum coherence in a system coupled to a zero-temperature environment*. *Eur. Phys. J. B*. 2005;46(2):519–528.
11. Martin Tchoffo, Georges Collince Fouokeng, et al. *Effect of the Variable B-Field on the Dynamic of a Central Electron Spin Coupled to an Anti-Ferromagnetic Qubit Bath*. *World Journal of Condensed Matter Physics*. 2012;(2):246-256.
12. Shannon CE. *A mathematical theory of communication*. *Bell Syst. Tech. J*. 1948;27(1):379–423 and 623–656.
13. Sagar RP, Hô M, Mex J. *Shannon Entropies of Atomic Basins and Electron Correlation Effects*. *Chem. Soc*. 2008;52(1):60-66.
14. Guo-Hua Sun, Shi-Hai Dong. *Phys. Scr*. 2013;87(4):045003.
15. Griffiths RB. *Types of Quantum Information*. *Phys. Rev. A*. 2007;76(6):062320-1-10.
16. Zurek WH. *Decoherence and the Transition from Quantum to Classical*. *Phys. Today*. 1991;44(10):36-44.
17. Martin Tchoffo, Georges Collince Fouokeng, et al. *Thermodynamic Properties and Decoherence of a Central Electron Spin of Atom Coupled to an Anti-Ferromagnetic Spin Bath*. *Journal of Quantum Information Science*. 2013;(3):10-15.
18. Özcan Ö, Aktürk E, Sever R. *Time Dependent Entropy of Constant Force Motion*. *Turk J. Phys*. 2007;31(1):191-196.
19. Cerf NJ, Adami C. *Negative entropy and information in quantum mechanics*. *Phys. Rev. Lett*. 1997;79(26):5194-5197.
20. Omnes R. *Consistent interpretations of quantum mechanics*. *Rev. Mod. Phys*. 1992;64(2):339.
21. Charis Anastopoulos. *Quantum probabilities versus event frequencies Brazilian Journal of Physics*. 2005;35(2B):503-508.

22. Eric M Heatwole, Oleg V. Prezhdo. Analytic dynamics of the Morse oscillator derived by semiclassical closures. *J. Chem. Phys.* 2009;130(24):244111-1-12.
23. Jörn Dunkel, Sergey A. Trigger. Time-dependent entropy of simple quantum model systems. *Phys. Rev. A.* 2005;71(5):052102-1-12.
24. Garbaczewski P. Comment on "Time-dependent entropy of simple quantum model systems". *Phys. Rev. A.* 2005;72(5):056101.
25. Zuo J, O'Connell RF. Effect of an external field on decoherence: Part II. *J. Mod. Opt.* 2004;51(6):821-832.
26. Gobert D, Delft JV. Comment on "Quantum measurement and decoherence". *Phys Rev. A.* 2004;70(2):026101-1-4.
27. Ford GW, Lewis JT, O'Connell RF. Quantum Measurement and Decoherence. *Phys Rev A.* 2001;64(3):032101-1-4.
28. Zurek WH. Decoherence, einselection, and the quantum origins of the classical. *Rev. Mod. Phys.* 2003;75(3):715–775.
29. Born M, *Phys Z.* The Adiabatic Principle in Quantum Mechanics. *Z. Phys.* 1926;40(4):167.
30. Feynman RP, Hibbs AR. *Quantum Mechanics and path integrals.* McGraw-Hill, USA; 1965.
31. Khandekar DC, Lawande SV, Bhagwat KV. *Path integrals Methods and Their Applications.* World scientific, Singapore; 1993.
32. Aslangul C, Pottier N, Saint-James D. Quantum ohmic dissipation: coherence vs. incoherence and symmetry-breaking. A simple dynamical approach. *J. Physique.* 1985;46(12):2031-2045.
33. Aly SH. Specific heat, Energy Fluctuation and Entropy of Isotropic Harmonic and Anharmonic Oscillators. *Egypt. J. Sol.* 2000;23(2):217-230.
34. Campisi M. Increase of Boltzmann entropy in a quantum forced harmonic oscillator. *Phys. Rev E.* 2008;78(5):051123-1-10.
35. Schreiber A, Cassemirino KN, Podoček V, Gábris A, Jex I, Silberhorn Ch. Decoherence and Disorder in Quantum Walks: From Ballistic Spread to Localization. *Phys. Rev. Lett.* 2011;106(18):180403-1-4.

© 2014 Fai et al.; This is an Open Access article distributed under the terms of the Creative Commons Attribution License (<http://creativecommons.org/licenses/by/3.0>), which permits unrestricted use, distribution, and reproduction in any medium, provided the original work is properly cited.

Peer-review history:

The peer review history for this paper can be accessed here:
<http://www.sciencedomain.org/review-history.php?iid=310&id=4&aid=2375>